LASER INTERFEROMETER GRAVITATIONAL WAVE OBSERVATORY
- LIGO -
CALIFORNIA INSTITUTE OF TECHNOLOGY
MASSACHUSETTS INSTITUTE OF TECHNOLOGY

Technical Note **LIGO-T1700322–v1** 2017/07/10

Searching for echoes of gravitational waves from coalescences of exotic compact objects

Ka-Lok Lo
Mentor: Alan Weinstein

California Institute of Technology
LIGO Project, MS 18-34
Pasadena, CA 91125
Phone (626) 395-2129
Fax (626) 304-9834
E-mail: info@ligo.caltech.edu

Massachusetts Institute of Technology
LIGO Project, Room NW22-295
Cambridge, MA 02139
Phone (617) 253-4824
Fax (617) 253-7014
E-mail: info@ligo.mit.edu

LIGO Hanford Observatory
Route 10, Mile Marker 2
Richland, WA 99352
Phone (509) 372-8106
Fax (509) 372-8137
E-mail: info@ligo.caltech.edu

LIGO Livingston Observatory
19100 LIGO Lane
Livingston, LA 70754
Phone (225) 686-3100
Fax (225) 686-7189
E-mail: info@ligo.caltech.edu

http://www.ligo.caltech.edu/

1 Motivation and Objective

In light of the results claimed in [4], we would like to verify their results using independent templates and methodologies. In this project, we aim to search for echoes of gravitational wave in the three detections LIGO had using matched filtering technique. We then perform a Bayesian analysis of parameter estimation and model selection on the triggers we found in the first stage of matched filtering search.

2 Background

Up to date, the Laser Interferometer Gravitational-wave Observatory (LIGO) has successfully detected three compact binary coalescence events: GW150914, GW151226, GW170104 [1, 2, 3]. These detections mark the beginning of a new era of gravitational-wave astronomy and astrophysics, where we can infer and probe the properties and structure of astronomical objects using gravitational-wave signals. Throughout the project, we will use geometrized unit $c = G = 1$.

2.1 Echoes of gravitational waves from coalescences of exotic compact objects

During the inspiral phase of gravitational wave emission from the coalescence of a compact binary system, say binary black hole system, the two black holes spiral towards each other with an increasing orbital frequency. Eventually, they coalesce in the merger phase to form one single black hole. The final black hole then relaxs to a stationary Kerr black hole during the ringdown phase. Figure 1 shows the numerical relativity simulation and the reconstructed template of the first detection.

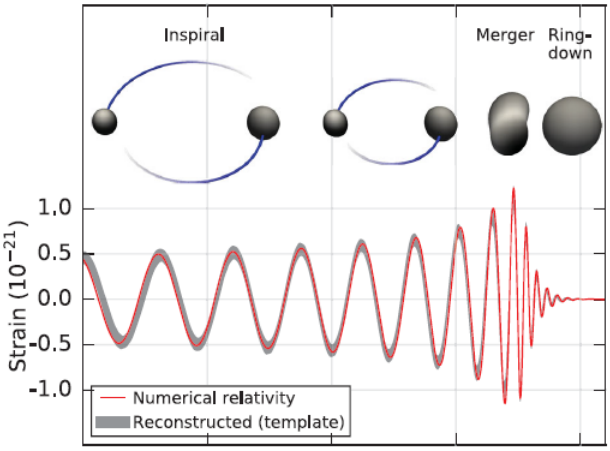

Figure 1: The numerical relativity simulation (in red) and reconstructed template (in gray) of GW150914. Figure taken from [2].

Cardoso, Franzin and Pani [7] first pointed out that the ringdown part of the gravitational wave can be used as a probe of the structure of a compact object. A very compact object, not necessary a black hole, with light ring will also exhibit similar ringdown as that of a black hole. Cardoso, Hopper, Macedo, Palenzuela and Pani [8] further showed that similar ringdown stage will also be exhibited for different types of **exotic compact objects** (ECOs) with light ring (or photon sphere), and there will be a train of echoes in the late-time ringdown phase associated with the photon sphere. Figure 2 shows an example of the aforementioned echoes in the ringdown phase.

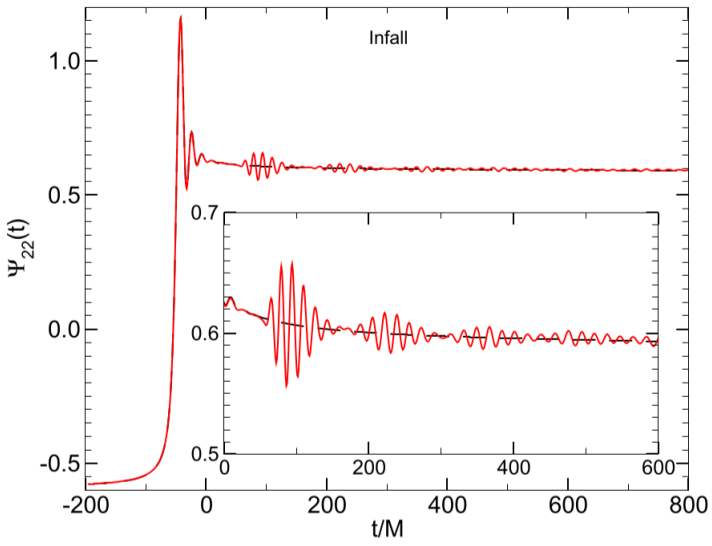

Figure 2: The waveform of a radially infalling particle into a wormhole (in red) compared to that into a black hole (in black). We can clearly see the train of echoes for the wormhole case, whereas this feature is absent for black hole. Figure taken from [8].

2.1.1 Previous endeavours of searching the echoes of gravitational waves

Abedi, Dykaar and Afshordi published a paper on December 2016, claiming that they have found evidence of Planck-scale structure near the black hole event horizons at a combined 2.9σ significance level [4] on GW150914, LVT151012 and GW151226 using matched filtering technique.

In their search, they model the echoes with 5 free parameters, with the phase change between each echo being -1. The description of these 5 parameters are tabulated in Table 1.

Using the notations in [4], the echo template $\mathcal{M}_{\rm TE,I}(t)$ in time-domain is given by

$$\mathcal{M}_{\rm TE,I}(t) \equiv A\sum_{n=0}^{\infty}(-1)^{n+1}\gamma^n\mathcal{M}_{\rm T,I}(t)(t+t_{\rm merger}-t_{\rm echo}-n\Delta t_{\rm echo},t_0), \qquad (1)$$

Parameter	Description
$\Delta t_{\rm echo}$	The time interval between each echo
$t_{\rm echo}$	The time of arrival of the first echo
t_0	The time of truncation of the GW CBC template $\mathcal{M}_{\rm I}(t)$ to produce the echo template $\mathcal{M}_{\rm TE,I}(t)$
γ	The damping factor
A	The (overall) amplitude of the echoes

Table 1: The five free parameters of templates used by Abedi et al. [4].

where $t_{\rm merger}$ is the time of merger and $\mathcal{M}_{\rm T,I}(t)$ is a smooth activation of the GW post-merger template given by

$$\begin{aligned}\mathcal{M}_{\rm T,I}(t) &\equiv \Theta(t,t_0)\mathcal{M}_{\rm I}(t)\\ &\equiv \frac{1}{2}\left\{1+\tanh\left[\frac{1}{2}\omega_{\rm I}(t)(t-t_{\rm merger}{}_{-t_0})\right]\right\}\mathcal{M}_{\rm I}(t).\end{aligned}$$

Here $\omega_{\rm I}(t)$ denotes the frequency evolution as a function of time [4].

A team of physicists in Max Planck Institute for Gravitational Physics (AEI) questioned the data analysis method in Abedi et al.'s paper[6] and Abedi et al. responded that the shortcomings pointed by them would only change the significance by less than 0.3σ [5].

Motivated by solving the linear perturbation with a completely reflective boundary condition around a Kerr black hole, Nakano, Sago, Tagoshi and Tanaka suggested a refined phenomenological template of echoes of gravitational wave [13]. In frequency-domain, the template of the $n^{\rm th}$ echo $\tilde{h}_n(f)$ is given by

$$\tilde{h}_n(f) = e^{-i(2\pi f\Delta t+\phi(f))(n-1)}(\sqrt{R(f)})^{n-1}\sqrt{1-R(f)}\tilde{h}(f), \tag{2}$$

where $\tilde{h}(f)$ is the Fourier transform of the waveform that reflects off the surface of ECO and $\phi(f)$ is the phase change when the gravitational wave was reflected at the potential barrier and at the boundary near horizon. The reflection rate, denoted by $\sqrt{R}$ in Eq.2, or reflection amplitude $\tilde{\mathcal{R}}_{\rm BH}$ (later defined in Eq.7), can be estimated using the fitting formulas in [13].

They also proposed two simple models of $h(t)$, the waveform that reflects off the surface of ECO, that we have just mentioned. The first model is given by

$$h_1(t) \propto \frac{e^{-i\omega_{\rm QNM}\tilde{t}}}{1+e^{-2\beta|\Im(\omega_{\rm QNM})|t}}, \tag{3}$$

where $\beta \ll 1$ is a model parameter to eliminate the high frequency tail [13] due to the implicit periodic assumption when using Discrete Fourier Transform, and $\tilde{t}$ gives the frequency evolution, which is given by

$$\frac{d\tilde{t}}{dt} = \frac{1}{1+e^{-2\alpha|\Im(\omega_{\rm QNM})|t}}. \tag{4}$$

As for the second model, it is given by

$$h_2(t) \propto \frac{e^{-i\omega_{\rm QNM}t}}{1+e^{-2\bar{\alpha}|\Im(\omega_{\rm QNM})|t}}. \tag{5}$$

The two parameters α and $\bar{\alpha}$ are for controlling the excitation of quasi-normal mode at QNM frequency $\omega_{\rm QNM}$ [13]. It should be noted that Nakano et al. claimed that the templates and reprocessing they proposed in [13] work in the context of gravitational-waves, namly

$$h(t) = h_+(t) + ih_\times(t),$$

where $h_+(t)$ and $h_\times(t)$ are the plus and cross polarization of gravitational waves respectively.

Recently, Mark, Zimmerman, Du and Chen published a paper about the echoes from ECOs [11]. They modelled an exotic compact object with a Schwarzchild metric in the exterior and a spherically symmetric metric in the interior, together with a reflective boundary condition on the ECO surface $x = x_0$ with a reflection amplitude $\tilde{\mathcal{R}}(\omega)$. Here x is the tortoise coordinate defined as

$$x = r + 2M\ln(\frac{r-2M}{M}).$$

They numerically calculated the scalar waves as observed by distant observers. They argued that the echo waveforms can be modulated from the waveform on the black hole horizon when there is no reflecting surface [11]. As such, they proposed a phenomenological template $Z_{\rm T}$ of the echoes from ECOs in frequency domain:

$$Z_{\rm T} = \tilde{K} Z_{\rm T}^{\rm H}, \tag{6}$$

where $Z_{\rm T}^{\rm H}$ is the horizon waveform template in frequency domain and $\tilde{K}$ is the transfer function, which contains most of the physics in this model. The transfer function $\tilde{K}(\omega)$, as a function of angular frequency ω, is given by

$$\tilde{K}(\omega) = \frac{\tilde{\mathcal{T}}_{\rm BH}\tilde{\mathcal{R}}e^{-2i\omega x_0}}{1-\tilde{\mathcal{R}}_{\rm BH}\tilde{\mathcal{R}}e^{-2i\omega x_0}}, \tag{7}$$

where $\tilde{\mathcal{T}}_{\rm BH}(\omega)$, $\tilde{\mathcal{R}}_{\rm BH}(\omega)$ are the transmission amplitude and reflection amplitude of the black hole respectively, using the notations in [11]. Note that

$$|\tilde{\mathcal{T}}_{\rm BH}|^2 + |\tilde{\mathcal{R}}_{\rm BH}|^2 = 1.$$

We can expand Eq.7 as a geometric series:

$$\tilde{K}(\omega) = \tilde{\mathcal{T}}_{\rm BH}\tilde{\mathcal{R}}e^{-2i\omega x_0}\sum_{n=1}^{\infty}(\tilde{\mathcal{R}}_{\rm BH}\tilde{\mathcal{R}})^{n-1}e^{-2i(n-1)\omega x_0}. \tag{8}$$

If we define the transfer function for the $n^{\rm th}$ echo as

$$\tilde{K}^{(n)} = (\tilde{\mathcal{T}}_{\rm BH}\tilde{\mathcal{R}})(\tilde{\mathcal{R}}_{\rm BH}\tilde{\mathcal{R}})^{n-1}e^{-2in\omega x_0}, \tag{9}$$

then we can write Eq.6 as a sequence of echoes

$$Z_{\rm T} = \sum_{n=1}^{\infty} Z_{\rm T}^{(n)} = \sum_{n=1}^{\infty} \tilde{K}^{(n)} Z_{\rm T}^{\rm H}.$$

The overall waveform observed by distant observers $Z_{\rm ref}^{\infty}$ is given by

$$Z_{\rm ref}^{\infty} = Z_{\rm BH}^{\infty} + \tilde{K} Z_{\rm BH}^{\rm H}.$$

Therefore, to generate a template for searching echoes, one just needs to add the reprocessed horizon template to the BH template in the frequency-domain.

Mark et al. observed that the ringdown of the horizon waveform determined the shape of the echoes. Hence, to get these features correct, Mark et al. proposed to use the following model [11]:

$$Z_{\rm T}^{\rm H}(\omega) = e^{i\omega t_s} e^{-\omega^2/(2\beta^2)} \left(\frac{\alpha_+}{\omega - \Omega_+} + \frac{\alpha_-}{\omega - \Omega_-} \right), \tag{10}$$

the meaning of the template parameters are tabulated in Table 2. Together with the number of echoes n, the surface of the ECO x_0 and assuming that the reflection amplitude $\tilde{\mathcal{R}}$ can be approximated by a constant, there are a total of 7 free parameters in this echo model.

Parameter	Description
α_+	The complex amplitude of the sinusoid at positive QNM frequency $\Omega_+ = \Omega_R + i\Omega_I$
α_-	The complex amplitude of the sinusoid at negative QNM frequency $\Omega_- = -\Omega_R + i\Omega_I$
t_s	The central start time of the Gaussian
β	The frequency width of the Gaussian

Table 2: The four free parameters of templates used by Mark et al. [11].

2.2 Searching for signals: Matched Filtering

In order to search for gravitational wave signals buried with noises, we can deploy matched filtering. The basic idea behind matched filtering is that we slide a pre-generated template across the signal and compare the two and repeat the above process for a large number of templates. For each comparison we compute a value known as **Signal to Noise Ratio** (SNR) ρ which can be intuitively defined as

$$\text{SNR} = \rho = \frac{\sqrt{\text{Power}_{\text{signal}}}}{\sqrt{\text{Power}_{\text{noise}}}}.$$

Suppose we are filtering the data $d(t)$ with some normalized templates $\{h_i^c(t)\}$, then the complex matched filtering response $z_i(t)$ is given by [12]

$$z_i(t) = x_i(t) + i y_i(t), \tag{11}$$

$$= 4 \int_0^{\infty} df \frac{\tilde{h_i^c}^*(f)\tilde{d}(f)}{S_n(f)} e^{2\pi i f t}, \tag{12}$$

where $x_i(t)$ and $y_i(t)$ are the matched filtering response to h_+ and $h_\times$ respectively and $S_n(f)$ is the power spectral density of noise. The SNR is simply the modulus of $z(t)$, namely

$$\text{SNR} = \rho(t) = |z(t)| \tag{13}$$

Higher the SNR, higher the similarity between the signal and the template. Since parameters of the signals that we are looking for are not known in advance, as a result we have to prepare a collection of hundreds of thousands of templates, called the template bank, that covers the parameter space we are searching for.

2.3 Bayesian Analysis and Hypothesis Testing

Bayesian analysis provides us a consistent framework of inductive logic. The central piece of the Bayeisan framework is the **Bayes' Theorem**, which allows us to update our degree of belief of a hypothesis H with a prior knowledge I when a new data d is available.

2.3.1 Bayes' Theorem

Mathematically, Bayes' theorem (also known as Bayes' rule) states that

$$\Pr(B|A) = \frac{\Pr(A|B)\Pr(B)}{\Pr(A)}, \tag{14}$$

where $\Pr(A)$ and $\Pr(B)$ denote the (discrete) probability of event A and event B occurs, regardless of each other, respectively; $\Pr(A|B)$ is the probability of event A **on the condition that** that event B occurs and likewise for $\Pr(B|A)$.

2.3.2 Parameter Estimation

Suppose we have a generative model H that describes the observed data d given some parameters $\vec{\theta} = (\theta_1, \theta_2, ..., \theta_n)$. Before the observation, suppose we already have some knowledge I about the parameters $\vec{\theta}$ assuming that the model H is true, represented by the **prior probability distribution** $p(\vec{\theta}|H, I)$, we can then use Eq.14 to update our knowledge or degree of belief of the value of these parameters to get the **posterior probability distribution** $p(\vec{\theta}|d, H, I)$ as follows:

$$p(\vec{\theta}|d, H, I) = \frac{p(d|\vec{\theta}, H, I)p(\vec{\theta}|H, I)}{p(d|H, I)} \tag{15}$$

$$= \frac{p(d|\vec{\theta}, H, I)p(\vec{\theta}|H, I)}{\int_\theta p(d|\vec{\theta'}, H, I)p(\vec{\theta'}|H, I)d\theta'}. \tag{16}$$

The term $p(d|\vec{\theta}, H, I)$, when viewed as a function of the parameters $\vec{\theta}$, is called the **likelihood** function and denoted as $\mathcal{L}(\vec{\theta}|d, H, I)$. As for the term $p(d|H, I)$, it is called the **evidence**, or marginal likelihood. In this scenairo, it can be considered as a normalization constant and often ignored. Then, Eq.15 can be turned into:

$$p(\vec{\theta}|d, H, I) \propto p(d|\vec{\theta}, H, I)p(\vec{\theta}|H, I). \tag{17}$$

2.3.3 Hypothesis Testing

Suppose we have two (generative) models H_0 and H_1, and we want to compare which model describes the observed data the best. It is useful to compute the **odds ratio** defined as

$$O_{H_0}^{H_1} = \frac{p(H_1|d,I)}{p(H_0|d,I)}. \tag{18}$$

Applying Eq.14 to Eq.18, we have

$$O_{H_0}^{H_1} = \frac{p(d|H_1,I)p(H_1|I)}{p(d|H_0,I)p(H_0|I)}.$$

The factor $\frac{p(H_1|I)}{p(H_0|I)}$ is called the **prior odds** and the factor $\frac{p(d|H_1,I)}{p(d|H_0,I)}$ is called the **Bayes factor**, denoted as $B_{H_0}^{H_1}$.

A question that arises naturally is that how can we compute the term $p(d|H_i,I)$, where $i = 0,1$. Suppose H_0 has no free parameter, whereas H_1 has n free parameters $\vec{\theta} = (\theta_1, \theta_2, ..., \theta_n)$. Then it is straightforward to calculate $p(d|H_0,I)$. But for $p(d|H_1,I)$, by re-arranging Eq.14 we have

$$p(\vec{\theta}|d,H_1,I)p(d|H_1,I) = p(d|\vec{\theta},H,I)p(\vec{\theta}|H_1,I).$$

Integrating both sides with respect to $\vec{\theta}$ (or *marginalizing over the parameters*), we have

$$\int p(\vec{\theta}|d,H_1,I)p(d|H_1,I)d\vec{\theta} = \int p(d|\vec{\theta},H_1,I)p(\vec{\theta}|H_1,I)d\vec{\theta}.$$

Note that $p(d|H_1,I)$ is independent of $\vec{\theta}$ and by definition

$$\int p(\vec{\theta}|d,H_1,I)d\vec{\theta} = 1,$$

We finally arrive at

$$p(d|H_1,I) = \int p(d|\vec{\theta},H_1,I)p(\vec{\theta}|H_1,I)d\vec{\theta}. \tag{19}$$

When the odds ratio $O_{H_0}^{H_1} > 1$, that means the observed data favours (alternative) hypothesis H_1 more than the hypothesis H_0 and vice versa.

One thing that we must be cautious about is that a model that fits the data best does not imply the model gives the highest evidence. A more complicated model (i.e. with more free parameters) often subjects to more noise than a simpler model (i.e. with less free parameters). This is similar to overfitting in regression. When you have N data points for fitting, you can always use a degree N polynomial to fit all points, but very likely the fitted polynomial will not generalize well to new data because it was affected by the noise in the data.

Bayesian analysis embodies the **Occam's razor** and penalizes more complicated model automatically. The following example was taken from [10]. Suppose there are two models

H_0 and H_1 with H_0 having no free parameter and H_1 having 1 free parameter θ. Assume that there is no prior knowledge to favour a particular model, i.e. the prior odds is simply 1. We further assume that the prior probability distribution for model H_1 is constant over a range $\theta \in [\theta_{\rm min}, \theta_{\rm max}]$, namely

$$p(\theta|H_1, I) = \begin{cases} \dfrac{1}{\theta_{\rm max} - \theta_{\rm min}}, & \theta \in [\theta_{\rm min}, \theta_{\rm max}] \\ 0, & \text{otherwise} \end{cases}.$$

We also assume that the likelihood to be a Gaussian function, centered around the maximum likelihood when $\theta = \theta_0$, with a standard deviation of σ_θ. Mathematically,

$$p(d|\theta, H_1, I) = p(d|\theta_0, H_1, I) e^{-\frac{(\theta-\theta_0)^2}{2\sigma_\theta^2}}.$$

The odds ratio can be found easily by integration:

$$O^{H_1}_{H_0} = \frac{p(d|\theta_0, H_1, I)}{p(d|H_0, I)} \frac{\sqrt{2\pi}\sigma_\theta}{\theta_{\rm max} - \theta_{\rm min}}.$$

Very often, the first factor $\dfrac{p(d|\theta_0, H_1, I)}{p(d|H_0, I)} > 1$, since often a more complicated model fits the data better than a simpler model. However, the second factor suggests that if the parameter θ is unnecessary to describe the data in a sense that the width of the likelihood function is much smaller than the width of the prior, i.e. $\sigma_\theta \ll \theta_{\rm max} - \theta_{\rm min}$, the second factor will penalize H_1 is a sense that the odds ratio will become smaller.

3 Progress

3.1 Implementing the template model

The template model described in [11] by Mark et al. was implemented in Python. Table 3 summarizes the five main functions in the implementation `phenom_echoes_waveform_tapir.py`. Figure 3 shows the horizon waveform as shown in Fig. 20 of [11], reproduced using our Python implementation, as a check that the implementation was done properly.

Function	Description
`get_fd_horizon_waveform`	Generate the horizon waveform in frequency-domain $Z^{\rm H}_{\rm T}$
`get_fd_total_transfer`	Compute the total transfer function $\tilde{K}$
`get_fd_nth_transfer`	Compute the $n^{\rm th}$ transfer function $\tilde{K}^{(n)}$
`get_fd_total_echoes`	Generate the total echo waveform in frequency-domain $Z_{\rm T}$
`get_fd_upto_n_echoes`	Generate the echo waveform up to $n^{\rm th}$ echo in frequency-domain $Z_{\rm T} = \sum_{k=1}^{n} Z^{(k)}_{\rm T}$

Table 3: The five main functions in the Python implemenation of templates described in Mark et al. [11].

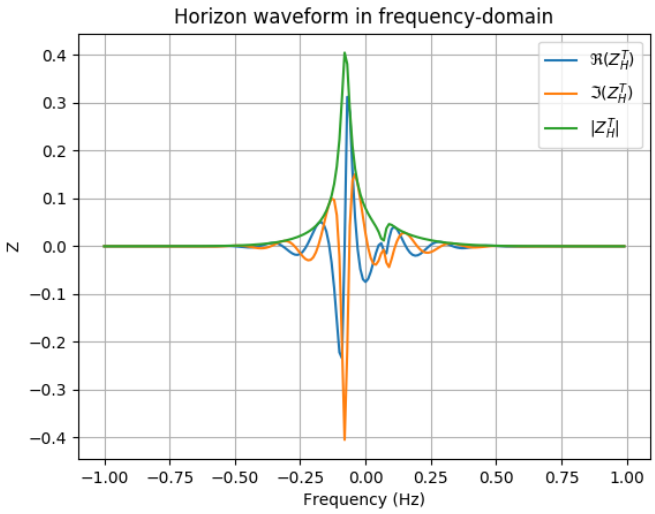

Figure 3: The horizon waveform as shown in Fig. 20 in [11], reproduced using our implementation.

3.2 Testing the nature of parameters of a template model

Before performing a matched filtering search, one must first build a template bank with templates of various parameters for the search. There are two kinds of parameters: intrinsic and extrinsic parameters. The extrinsic parameters would only scale the template but not its shape, and thus they can be kept fixed during a matched filtering search so as to reduce the dimensionality of the search and speed up the search. However, for intrinsic parameters, changing their values would also change the shape of a template, and therefore we must vary these parameters in the template bank. For example, the component masses m_1, m_2 and component spins $\vec{S}_1 = (S_{1,x}, S_{1,y}, S_{1,z})$, $\vec{S}_2 = (S_{2,x}, S_{2,y}, S_{2,z})$ are intrisnic parameters of a GW CBC template, whereas parameters such as luminosity distance d and phase ϕ are extrisnic parameters. Figure 4(a) and 4(b) show two templates with different luminosity distances. We can see that they only differ each other by the amplitude.

4 Challenges and Problems encountered

4.1 Computing the reflection amplitude $\tilde{\mathcal{R}}_{\mathrm{BH}}(\omega)$ and transmission amplitude $\tilde{\mathcal{T}}_{\mathrm{BH}}(\omega)$

In both Nakano et al.'s and Mark et al.'s models, there are two quantities that are required: reflection amplitude $\tilde{\mathcal{R}}_{\mathrm{BH}}(\omega)$ in Mark et al.'s notation or $\sqrt{R}$ in Nakano's notation, and transmission amplitude $\tilde{\mathcal{T}}_{\mathrm{BH}}(\omega)$ in Mark et al.'s notation or $\sqrt{1-R}$ in Nakano's notation. From now on, we will use Mark et al.'s notations for the sake of clarity and consistency.

In Nakano et al.'s paper, there are two fitting formulas for $\tilde{\mathcal{R}}_{\mathrm{BH}}$, one for positive and one for negative frequencies f. In practice, we would like to compute the reflection amplitude

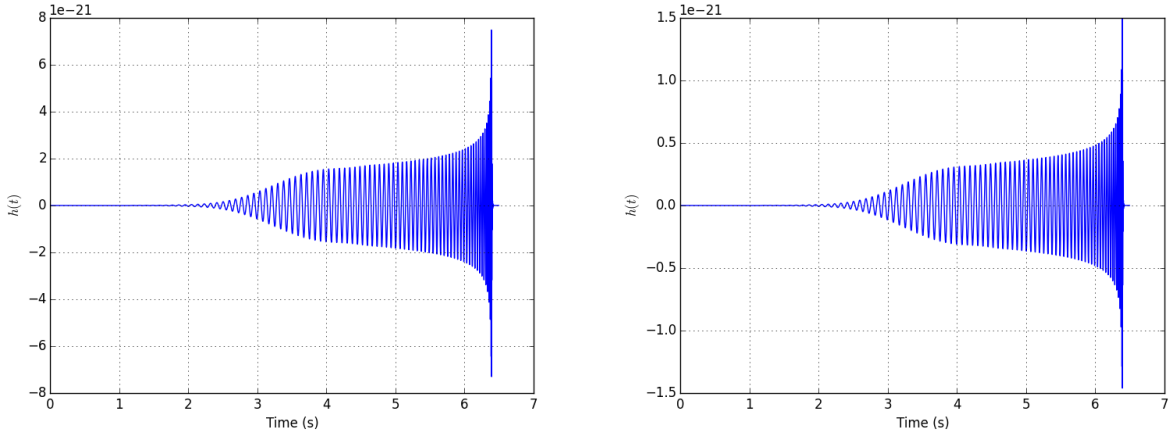

(a) Luminosity distance $d = 100$ Mpc

(b) Luminosity distance $d = 500$ Mpc

Figure 4: IMRPhenomPv2 template of two gravitaional-wave signals, differing only by their luminosity distance. We can clearly see that the two signals have the same form and 4(a) is just a scaled-up version of 4(b) since it is closer to us.

(and hence transmission amplitude by the normalization condition) for each of the systems LIGO had detected. For now, we will be using Nakano et al.'s fit for testing purposes to build the infrastructure of the search pipeline first.

4.2 Using the templates in the context of GW

In Section 2.1.1, we mentioned that Nakano et al. argued that their templates work in the context of gravitational waves. However, attention must be paid when using the template proposed by Mark et al., since they derived the results in the context of scalar waves, whereas gravitational waves are metric perturbations from Minkowski spacetime $h_{\mu\nu} = g_{\mu\nu} - \eta_{\mu\nu}$. Also, the template was derived using a Schwarzchild spacetime, but the sources of LIGO's three detections are all rotating instead of static. Therefore, the template becomes a phenomenlogical model when we try to extend it to the case of gravitational waves from rotating ECOs.

4.3 Negative frequencies

In both Nakano et al.'s and Mark et al.'s models, the frequency f or angular frequency ω are allowed from negative infinity to positive infinity. This is a problem since we do matched filtering in a physical frequency range $f \in [f_{\text{low}}, f_{\text{high}}]$, where $f_{\text{low}} \geq 0$. To solve issue with Mark et al.'s model, we constraint the complex amplitudes $\alpha_{\pm}$ in the horizon waveform Z^{H}_{T} such that

$$Z^{\text{H}}_{\text{T}}(\omega)^* = Z^{\text{H}}_{\text{T}}(-\omega).$$

This implies that the horizon waveform in time-domain $\psi^{\text{H}}_{\text{T}}(t)$ is real and the negative frequency components in Fourier Transform are redundant. By noting that

$$\Omega^*_{\pm} = -\Omega_{\mp},$$

and some simple algebraic manipulations show that this can be achieved by rewriting $\alpha_\pm$ in terms of α_R and α_I:

$$\alpha_+ = \alpha_R + i\alpha_I, \tag{20}$$
$$\alpha_- = \alpha_R - i\alpha_I. \tag{21}$$

5 Tentative Plans, Prospective challenges and problems

5.1 Generating a template bank

5.1.1 Plan

After we have a working approximant of the echo waveform, we can then move on to generate a template bank for the matched filtering search. In this stage, we would have to define the parameter space of the search, meaning that we would have to set some (physical) limits on the values of the template parameters. We would also need to modify one of the search pipelines used by LIGO, `PyCBC`, so that we can utilize it to generate an effectual template bank, and the effectualness [9] or fitting factor of the bank will be measured using many injected signals with `banksim`.

5.1.2 Prospective challenges and problems

A prospective problem for generating an effectual template bank is that the existing template placement algorithm may not work well for our echo templates to achieve the requirement of having a minimum overlap of 0.97 with any template in the bank.

5.2 Matched filtering search

5.2.1 Plan

After we have an effectual template bank, we can then move on to perform the actual searches on the three events using matched filtering. We would also need to perform background estimation to estimate the significance of the triggers.

6 Acknowledgement

The author would like to express his gratitude to Zachary Mark, the first author of [11], for his help and the friutful discussions of the project. The author would also like to thank Hiroyuki Nakano, the first author of [13] for his swift and constructive replies to the author's enquiries.

References

[1] B. P. Abbott et al. Gw151226: Observation of gravitational waves from a 22-solar-mass binary black hole coalescence. *Phys. Rev. Lett.*, 116:241103, Jun 2016.

[2] B. P. Abbott et al. Observation of gravitational waves from a binary black hole merger. *Phys. Rev. Lett.*, 116:061102, Feb 2016.

[3] B. P. Abbott et al. Gw170104: Observation of a 50-solar-mass binary black hole coalescence at redshift 0.2. *Phys. Rev. Lett.*, 118:221101, Jun 2017.

[4] J. Abedi, H. Dykaar, and N. Afshordi. Echoes from the Abyss: Evidence for Planck-scale structure at black hole horizons. *ArXiv e-prints*, December 2016.

[5] J. Abedi, H. Dykaar, and N. Afshordi. Echoes from the Abyss: The Holiday Edition! *ArXiv e-prints*, January 2017.

[6] G. Ashton, O. Birnholtz, M. Cabero, C. Capano, T. Dent, B. Krishnan, G. D. Meadors, A. B. Nielsen, A. Nitz, and J. Westerweck. Comments on: "Echoes from the abyss: Evidence for Planck-scale structure at black hole horizons". *ArXiv e-prints*, December 2016.

[7] V. Cardoso, E. Franzin, and P. Pani. Is the Gravitational-Wave Ringdown a Probe of the Event Horizon? *Physical Review Letters*, 116(17):171101, April 2016.

[8] V. Cardoso, S. Hopper, C. F. B. Macedo, C. Palenzuela, and P. Pani. Gravitational-wave signatures of exotic compact objects and of quantum corrections at the horizon scale. *Physical Review D*, 94(8):084031, October 2016.

[9] Thibault Damour, Bala R. Iyer, and B. S. Sathyaprakash. Improved filters for gravitational waves from inspiraling compact binaries. *Phys. Rev. D*, 57:885–907, Jan 1998.

[10] Tjonnie G F Li. *Extracting Physics from Gravitational Waves Testing the Strong-field Dynamics of General Relativity and Inferring the Large-scale Structure of the Universe*. Springer International Publishing, 1 edition, 2015.

[11] Z. Mark, A. Zimmerman, S. M. Du, and Y. Chen. A recipe for echoes from exotic compact objects. *ArXiv e-prints*, June 2017.

[12] C. Messick, K. Blackburn, P. Brady, P. Brockill, K. Cannon, R. Cariou, S. Caudill, S. J. Chamberlin, J. D. E. Creighton, R. Everett, C. Hanna, D. Keppel, R. N. Lang, T. G. F. Li, D. Meacher, A. Nielsen, C. Pankow, S. Privitera, H. Qi, S. Sachdev, L. Sadeghian, L. Singer, E. G. Thomas, L. Wade, M. Wade, A. Weinstein, and K. Wiesner. Analysis Framework for the Prompt Discovery of Compact Binary Mergers in Gravitational-wave Data. *ArXiv e-prints*, April 2016.

[13] H. Nakano, N. Sago, H. Tagoshi, and T. Tanaka. Black hole ringdown echoes and howls. *ArXiv e-prints*, April 2017.